Pseudogaps and Emergence of Coherence in Two-Dimensional Electron Liquids in SrTiO_{3}

Patrick B. Marshall, Evgeny Mikheev, Santosh Raghavan, and Susanne Stemmer

Phys. Rev. Lett. **117**, 046402 — Published 22 July 2016

DOI: 10.1103/PhysRevLett.117.046402

Pseudogaps and Emergence of Coherence in Two-Dimensional Electron Liquids in $SrTiO_3$

Patrick B. Marshall, Evgeny Mikheev, Santosh Raghavan, and Susanne Stemmer*

Materials Department, University of California, Santa Barbara, CA 93106-5050, U.S.A.

* Corresponding author. E-mail: stemmer@mrl.ucsb.edu

Abstract

Using tunneling spectroscopy we show that pseudogaps emerge in strongly correlated, two-dimensional electron liquids in $SrTiO_3$ quantum wells that are tuned near a quantum critical point. Coherence peaks emerge at low temperatures in quantum wells embedded in antiferromagnetic $SmTiO_3$ that remain itinerant to the lowest thickness. Quantum wells embedded in ferrimagnetic $GdTiO_3$ that become ferromagnetic at low temperatures show no indication of quasiparticle coherence. They undergo a symmetry-lowering metal-to-insulator transition at the lowest thicknesses that coincides with a vanishing single-particle density of states (DOS) around the Fermi level. Both types of quantum wells show a power-law depletion of the DOS at high energies. The results show that the different pseudogap behaviors are closely correlated with the type of magnetism in the proximity of the quantum wells, and thus provide insights into the microscopic mechanisms.

Pseudogaps are a reduction of the single particle spectral weight around the Fermi level and are a hallmark of strongly correlated systems that are near quantum critical points or unusual types of order. They have been observed in high-temperature superconductors [1-7], heavy-fermion compounds [8], charge density wave systems [9, 10], rare-earth nickelates [11], and even cold atom systems [12]. While pseudogaps in many correlated materials are still not fully understood [3-5, 13], they provide unique information about electron correlation physics. Tunneling and photoemission measurements of pseudogaps probe the degree to which the low-energy excitations of an interacting electron liquid differ from those of a Fermi gas. Features above the gap contain information about quantum phase fluctuations and the emergence of coherence. Conversely, systematic manipulation of critical behavior and dimensionality can yield new insights into *which* critical fluctuations give rise to pseudogaps and how new ordered states emerge. Additionally, disorder can play a strong role in correlated electron systems, and can produce observable anomalies in tunneling, such as zero-bias anomalies (ZBAs) in the metallic phase [14] and Coulomb gaps deep in the insulating state [15-17]. Disentangling the effects of disorder, electron-electron, and electron-lattice interactions, and understanding their effects on low energy excitations is critical to advancing the understanding of correlated materials.

Here, we study these questions in a strongly correlated low-dimensional electron system, namely two-dimensional electron liquids (2DELs) in narrow $SrTiO_3$ quantum wells, which are confined between insulating $RTiO_3$ barriers (R = Sm or Gd), see Fig. 1(a). The 2DELs in these quantum wells offer relative simplicity and tunability, while at the same time exhibiting the phenomena that have become hallmarks of strongly correlated systems, in particular, magnetism [18], metal-insulator transitions [19], non-Fermi liquid behavior [20, 21] and transport lifetime

separation [21]. These phenomena are tuned by the thickness of the quantum wells [specified by the number of SrO planes, see Fig. 1(a)] *and* by proximity to ferrimagnetic/antiferromagnetic Mott insulating RTiO$_3$. Specifically, for R = Sm (antiferromagnet), the quantum wells remain itinerant even when their thickness is reduced to a single SrO layer [21, 22]. The temperature dependence of the resistance ($R \sim AT^n$) changes from $n \sim 2$ to $n \sim 5/3$ below 5 SrO layers [20, 21]. For R = Gd (ferrimagnet), 2DELs become ferromagnetic below 10 K at 5 SrO layers [23], n remains Fermi liquid-like ($n \sim 2$). They undergo a metal-insulator transition at 2 SrO layers [19] that is accompanied by a lowering of the symmetry [22, 24]. Theory describes the insulating state as a dimer Mott insulator [25, 26] or a charge or orbital ordered insulator [26-29]. The electronic and magnetic states are summarized in Fig. 1(b). In analogy with other itinerant carrier systems that are tuned about a quantum critical point or are near a Mott transition [5], one may expect to observe pseudogaps and/or charge gaps.

Here, we use tunneling spectroscopy to probe the single particle density of states (DOS) in these 2DELs. We show that pseudogaps appear and that they evolve differently, both as a function of quantum well thickness and with temperature, depending on the specific instabilities near the quantum critical point. The results allow for insights into the low-energy excitations in strongly 2DELs when disorder, electron-electron interactions, magnetic fluctuations, and electron-lattice coupling are all present.

Figure 1(a) shows a schematic of the device, which employs epitaxial, wide band gap $SrZrO_3$ as the tunnel barrier. $SrZrO_3$/RTiO$_3$/$SrTiO_3$/RTiO$_3$ (R = Sm or Gd) structures were grown by hybrid molecular beam epitaxy (MBE) on single crystal $(LaAlO_3)_{0.3}(Sr_2AlTaO_6)_{0.7}$ (LSAT), as described in detail elsewhere [19, 22]. For the quantum well atomic structure, see refs. [22, 24]. All $SrTiO_3$ wells contain mobile carrier densities of $\sim 7\times10^{14}$ cm^{-2} [19, 21].

Tunnel devices were fabricated using two photolithography steps. Pt top contacts (100×350 μm^2) were deposited by e-beam evaporation. Ohmic contacts to the 2DEL were formed by using a buffered HF solution to etch through the $SrZrO_3$, followed by the deposition of a 40 nm thick layer of titanium. 400 nm thick gold pads were deposited on top of the titanium to facilitate wire bonding. Current-voltage (*I-V*) measurements were performed using a Keithley 2400 source meter by applying a voltage-controlled bias to the platinum top contact in a Quantum Design Physical Property Measurement System (PPMS) at temperatures ranging from 2 to 300 K. Multiple *I-V* curves using different sweep rates, directions, and bias ranges were collected to ensure reproducibility of the results. The Ohmic nature of the Ti contacts was verified for temperatures between 2 – 300 K [30]. Differential conductance spectra, d*I*/d*V* vs. *V* were obtained by numerical differentiation.

Figures 2(a-c) show differential conductance spectra, d*I*/d*V* vs. *V*, as a function of temperature and quantum well thickness for the quantum wells in $SmTiO_3$. At low temperatures, a nearly symmetric reduction of the DOS around the Fermi level (zero bias) is seen in all samples. The onset temperature and pseudogap shape depend on the quantum well thicknesses, with more pronounced reductions of the DOS in thinner quantum wells. The energy dependence of the DOS (conductance) in the 2 and 5 SrO thick quantum wells at energies above ~ 70 meV can approximately be described by power laws with exponents *m* near 0.4, as seen by the linear region in the log-log plots shown in Fig. 3 (a slight deviation from power law behavior may appear in the 2 SrO sample). The pseudogap (emerging at energies below 70 meV) does not follow a well-defined power law.

To better reveal changes in the DOS and clarify the low energy pseudogap, we show in Fig. 4 the normalized conductance, $d\ln(I)/d\ln(V) \sim (dI/dV)(I/V)^{-1}$. The use of the normalized

conductance minimizes contributions that vary slowly with V [31-34]. Note that $(dI/dV)(I/V)^{-1}$ is unity at $V = 0$ and thus only shows the relative depletion of the DOS, which we scale in Fig. 4 relative to the value at $V = 200$ meV. The small discontinuity at 0 V is due to the differentiation. In the 2 SrO layer quantum well, the pseudogap emerges below 200 K and coherence peaks are clearly visible at 10 K and below. With decreasing temperature, the pseudogap deepens, as already seen from Fig. 2(a), and states start to fill in just outside of the minimum – this eventually gives rise to the coherence peaks near an energy of 33 meV on either side of the gap. The pile up of DOS is visible as a kink in the dI/dV spectrum in Fig. 2(a) and thus not an artifact from the normalization. The coherence peaks allow us to estimate the energy scale of the pseudogap, 2Δ, of approximately 65 meV. For the 5 SrO quantum well, the onset temperature for the pseudogap is ~20 K. At 2 K we see a similar shape, namely an increase in the single particle DOS just outside of the minimum, i.e., precursors to coherence peaks. At 10 SrO layers the normalized DOS is featureless over the entire energy range, demonstrating how the normalized conductance removes the broad power law DOS behavior and clarifies resonant features in the DOS. The energy dependence of the DOS at high energies is also weaker.

Figures 2(d-f) show dI/dV vs. V for quantum wells in $GdTiO_3$. A full gap appears at 2 SrO layers, and is nearly temperature independent, consistent with the insulating ($dR/dT < 0$) nature of the in-plane sheet resistance [19]. Note that the DOS goes to zero at the Fermi level, unlike for any of the pseudogaps. A suppression of the DOS at low temperatures is observed for the 5 SrO quantum wells but shows a more featureless, V-like shape than that in the 5 SrO quantum well in $SmTiO_3$. Power law behavior with an exponent m near 0.3 is seen at higher energies, similar to the quantum wells in $SmTiO_3$. Comparison of $d\ln(I)/d\ln(V)$ at 2 K (Fig. 5), shows more clearly that, unlike for the 5 SrO quantum wells in $SmTiO_3$, no pile up of states

occurs outside the gap. A weak, ZBA-like feature also occurs for the 10 SrO layer thick quantum wells in $GdTiO_3$.

We next discuss the similarities and differences between the two types of quantum wells. The conductance spectra of both types feature pseudogaps, which appear as a symmetric suppression of the DOS around the Fermi level, as well as a power law DOS behavior at higher energies (above ~70 meV). Power laws appear in disordered systems with Coulomb interactions near the metal-insulator transition [17]. However, the in-plane sheet resistance of the *metallic* quantum wells is below 400 Ω/sq. at 2 K [21, 22], i.e. they are too far in the metallic state for Coulomb gap theory to apply. One may speculate that this may be an indicator of an unconventional metallic phase. Prior transport studies indicate that none of the 2DELs are Fermi liquids, *even when* $n \sim 2$ [21, 35]. Out of the power-law "backbone DOS" [17] pseudogaps emerge below ~ 5 SrO layers in both types of quantum wells.

The difference between the two types of quantum wells lies in how the depletion of the states evolves with temperature. For the thin quantum wells with $SmTiO_3$ barriers, with decreasing temperature, the loss of spectral weight at the Fermi level is accompanied by a pile up of states just outside the pseudogap, which is similar to what is seen in BCS superconductors, density wave systems, but not necessarily in all pseudogaps in the cuprates [36, 37]. In the thinnest well, an emerging coherent state appears at the lowest temperature, as evidenced by the coherence peaks. These features and the proximity to the antiferromagnetic $SmTiO_3$ make an itinerant antiferromagnetic state the most likely explanation. At high temperatures, this state is preceded by a loss of spectral weight without coherence. In contrast, the itinerant, ferromagnetic quantum wells in $GdTiO_3$ show no indication of conservation of states at low temperatures even though a pseudogap appears at a similar thickness. Reducing the thickness causes a symmetry

lowering transition to an insulator with a wide gap in the excitation spectrum and insulating behavior in the in-plane sheet resistance. This pseudogap is a crossover phenomenon to the incoherent insulator.

It is interesting to speculate on the implications for pseudogaps in other correlated materials. First, these pseudogaps are clearly unrelated to superconductivity. Secondly, the differences between the two types of quantum wells show that spin physics plays a critical role in the pseudogap. Spin fluctuations can give rise to pseudogaps [38]. A recent dynamical mean field study of quantum wells in $SmTiO_3$ found a loss in spectral weight associated with coupling of the 2DEL electrons to the antiferromagnetic fluctuations in the $SmTiO_3$ barrier [39]. In general, antiferromagnetic fluctuations affect only parts of the Fermi surface, whereas the ferromagnetic fluctuations affect the entire Fermi surface. Coherence may then emerge in the former case as the low temperature and the partial gapping reduce the phase space for scattering [38]. More generally, taking into account the symmetry lowering transition that occurs in the quantum wells in $GdTiO_3$, the results also support the idea that the strengths of electron-phonon interactions and repulsive Coulomb forces are influenced by magnetism [40] and the results show that this is expressed in the evolution of the pseudogaps. Specifically, the evolution of the pseudogap in the quantum wells in $SmTiO_3$ is quite typical of correlated electron systems, whereas that in $GdTiO_3$ appears to be dominated by the transition to a symmetry broken, gapped state, i.e., reflecting a stronger interaction with the lattice. Finally, we wish to again emphasize the incompatibility of all the transport properties of these quantum wells with Fermi liquid theory (carrier-density independent scattering rates, separation of Hall and longitudinal transport lifetimes [21, 35]). This supports the idea that the pseudogaps are an intrinsic manifestation of an unusual metallic state in a wider class of correlated electron systems.

Acknowledgments

The authors thank Frank Lechermann, Boris Shklovskii, Jim Allen, and Leon Balents for helpful discussions. This work was in part supported by the Center for Low Energy Systems Technology (LEAST), one of six centers of STARnet, a Semiconductor Research Corporation program sponsored by MARCO and DARPA, and by the U.S. Army Research Office (grant no. W911NF-14-1-0379). S. R. acknowledges support by the UCSB MRL, supported by the MRSEC Program of the NSF under Award No. DMR 1121053. P. B. M. also acknowledges support through an NSF Graduate Fellowship.

References

[1] H. Ding, T. Yokoya, J. C. Campuzano, T. Takahashi, M. Randeria, M. R. Norman, T. Mochiku, K. Kadowaki, and J. Giapintzakis, Nature **382**, 51 (1996).

[2] A. G. Loeser, Z. X. Shen, D. S. Dessau, D. S. Marshall, C. H. Park, P. Fournier, and A. Kapitulnik, Science **273**, 325 (1996).

[3] T. Timusk, and B. Statt, Rep. Progr. Physics **62**, 61 (1999).

[4] A. A. Kordyuk, Low Temp. Phys. **41**, 319 (2015).

[5] P. A. Lee, N. Nagaosa, and X.-G. Wen, Rev. Mod. Phys. **78**, 17 (2006).

[6] M. Randeria, in *Proceedings of the International School of Physics "Enrico Fermi" Course CXXXVI on High Temperature Superconductors*, edited by G. Iadonisi, J. R. Schrieffer, and M. L. Chiafalo (IOS Press, Amsterdam, 1998), pp. 53

[7] T. Shimojima, T. Sonobe, W. Malaeb, K. S. A. Chainani, A. Chainani, S. Shin, T. Yoshida, S. Ideta, A. Fujimori, H. Kumigashira, K. Ono, Y. Nakashima, H. Anzai, M. Arita, A. Ino, H. Namatame, M. Taniguchi, M. Nakajima, S. Uchida, Y. Tomioka, T. Ito, K. Kihou, C. H. Lee, A. Iyo, H. Eisaki, K. Ohgushi, S. Kasahara, T. Terashima, H. Ikeda, T. Shibauchi, Y. Matsuda, and K. Ishizaka, Phys. Rev. B **89**, 045101 (2014).

[8] V. A. Sidorov, M. Nicklas, P. G. Pagliuso, J. L. Sarrao, Y. Bang, A. V. Balatsky, and J. D. Thompson, Phys. Rev. Lett. **89**, 157004 (2002).

[9] P. A. Lee, T. M. Rice, and P. W. Anderson, Phys. Rev. Lett. **31**, 462 (1973).

[10] K. Rossnagel, J. Phys.: Condens. Matter **23**, 213001 (2011).

[11] S. J. Allen, A. J. Hauser, E. Mikheev, J. Y. Zhang, N. E. Moreno, J. Son, D. G. Ouellette, J. Kally, A. Kozhanov, L. Balents, and S. Stemmer, APL Mater. **3**, 062503 (2015).

[12] M. Feld, B. Fröhlich, E. Vogt, M. Koschorreck, and M. Köhl, Nature **480**, 75 (2011).

[13] M. R. Norman, D. Pines, and C. Kallin, Adv. Phys. **54**, 715 (2005).

[14] B. L. Altshuler, and A. G. Aronov, Solid State Comm. **30**, 115 (1979).

[15] A. L. Efros, and B. I. Shklovskii, J. Phys. C **8**, L49 (1975).

[16] E. I. Levin, V. L. Nguen, B. I. Shklovsii, and A. L. Efros, Sov. Phys. JETP **65**, 842 (1987).

[17] M. Lee, J. G. Massey, V. L. Nguyen, and B. I. Shklovskii, Phys. Rev. B **60**, 1582 (1999).

[18] C. A. Jackson, and S. Stemmer, Phys. Rev. B **88**, 180403(R) (2013).

[19] P. Moetakef, C. A. Jackson, J. Hwang, L. Balents, S. J. Allen, and S. Stemmer, Phys. Rev. B. **86**, 201102(R) (2012).

[20] C. A. Jackson, J. Y. Zhang, C. R. Freeze, and S. Stemmer, Nat. Commun. **5**, 4258 (2014).

[21] E. Mikheev, C. R. Freeze, B. J. Isaac, T. A. Cain, and S. Stemmer, Phys. Rev. B **91**, 165125 (2015).

[22] J. Y. Zhang, C. A. Jackson, R. Chen, S. Raghavan, P. Moetakef, L. Balents, and S. Stemmer, Phys. Rev. B **89**, 075140 (2014).

[23] P. Moetakef, J. R. Williams, D. G. Ouellette, A. P. Kajdos, D. Goldhaber-Gordon, S. J. Allen, and S. Stemmer, Phys. Rev. X **2**, 021014 (2012).

[24] J. Y. Zhang, J. Hwang, S. Raghavan, and S. Stemmer, Phys. Rev. Lett. **110**, 256401 (2013).

[25] R. Chen, S. Lee, and L. Balents, Phys. Rev. B **87**, 161119(R) (2013).

[26] D. Doennig, and R. Pentcheva, Sci. Rep. **5**, 79090 (2015).

[27] L. Bjaalie, A. Janotti, B. Himmetoglu, and C. G. Van de Walle, Phys. Rev. B **90**, 195117 (2014).

[28] F. Lechermann, and M. Obermeyer, New J. Phys. **17**, 043026 (2015).

[29] R. Pentcheva, and W. E. Pickett, Phys. Rev. Lett. **99**, 016802 (2007).

[30] See supplementary information [URL to be inserted by publisher] for the I-V measurements of the Ohmic contacts, .

[31] R. M. Feenstra, J. A. Stroscio, and A. P. Fein, Surface Sci. **181**, 295 (1987).

[32] J. A. Stroscio, R. M. Feenstra, and A. P. Fein, Phys. Rev. Lett. **57**, 2579 (1986).

[33] N. D. Lang, Phys. Rev. B **34**, 5947 (1986).

[34] R. J. Hamers, in *Scanning Tunneling Microscopy and Spectroscopy*, edited by D. A. Bonnell (VCH Verlagsgesellschaft, Weinheim, 1993), pp. 51.

[35] E. Mikheev, S. Raghavan, J. Y. Zhang, P. B. Marshall, A. P. Kajdos, L. Balents, and S. Stemmer, Sci. Rep. **6**, 20865 (2016).

[36] D. N. Basov, E. J. Singley, and S. V. Dordevic, Phys. Rev. B **65**, 054516 (2002).

[37] U. Chatterjee, J. Zhao, M. Iavarone, R. Di Capua, J. P. Castellan, G. Karapetrov, C. D. Malliakas, M. G. Kanatzidis, H. Claus, J. P. C. Ruff, F. Weber, J. van Wezel, J. C. Campuzano, R. Osborn, M. Randeria, N. Trivedi, M. R. Norman, and S. Rosenkranz, Nat. Comm. **6**, 6313 (2015).

[38] J. Schmalian, D. Pines, and B. S.́, Phys. Rev. B (in press) **60**, 667 (1999).

[39] F. Lechermann, unpublished.

[40] G. Sangiovanni, O. Gunnarsson, E. Koch, C. Castellani, and M. Capone, Phys. Rev. Lett. **97**, 046404 (2006).

Figure Captions

Figure 1: (a) Schematic of the tunnel device structure. The thickness of the $SrTiO_3$ quantum well is specified in terms of the number of SrO layers it contains – the example shown here contains two SrO layers, or one unit cell of $SrTiO_3$. (b) Phase diagram of the electronic and magnetic states in $GdTiO_3/SrTiO_3/GdTiO_3$ (top) and $SmTiO_3/SrTiO_3/SmTiO_3$ (bottom) quantum wells as a function of the $SrTiO_3$ well thickness, summarizing the results from both prior [18-21, 23] as well as this study.

Figure 2: Conductance spectra (dI/dV vs. V) as a function of temperature. Shown are data for $SrTiO_3$ quantum wells in $SmTiO_3$ (top row) and $GdTiO_3$ (bottom row). The thickness of the quantum wells is indicated in the figures.

Figure 3: Conductance spectra (dI/dV vs. V) at 2 K on a log-log scale. Results from the 2 SrO thick quantum well in $SmTiO_3$ and the 5 SrO thick quantum wells in $SmTiO_3$ and $GdTiO_3$ are shown. The dashed line indicates the approximate energy where the conductance deviates from the power law behavior at low energies.

Figure 4: Normalized conductance spectra ($d\ln(I)/d\ln(V)$ vs. V) at different temperatures for $SrTiO_3$ quantum wells in $SmTiO_3$. The thickness of the quantum wells is indicated in the figures. All $d\ln(I)/d\ln(V)$ values are shown relative to their value at 200 mV.

Figure 5: Normalized conductance spectra ($d\ln(I)/d\ln(V)$ vs. V) at 2 K for 2-SrO and 5-SrO quantum wells in $SmTiO_3$ and a 5-SrO quantum well in $GdTiO_3$. All $d\ln(I)/d\ln(V)$ values are shown relative to their value at 300 mV.

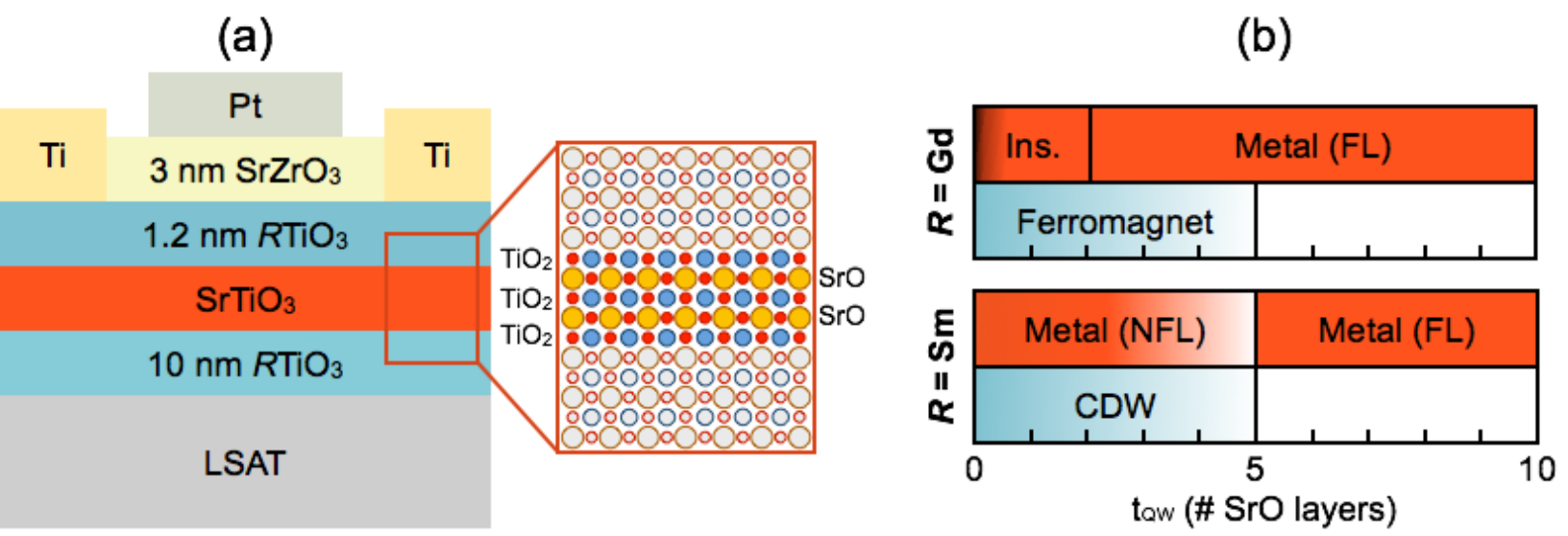
(a)
Pt
Ti
3 nm SrZrO3
Ti
1.2 nm RTiO3
SrTiO3
10 nm RTiO3
LSAT
TiO2
TiO2
TiO2
SrO
SrO
(b)
R = Gd
Ins.
Metal (FL)
Ferromagnet
R = Sm
Metal (NFL)
Metal (FL)
CDW
0
5
10
tQW (# SrO layers)

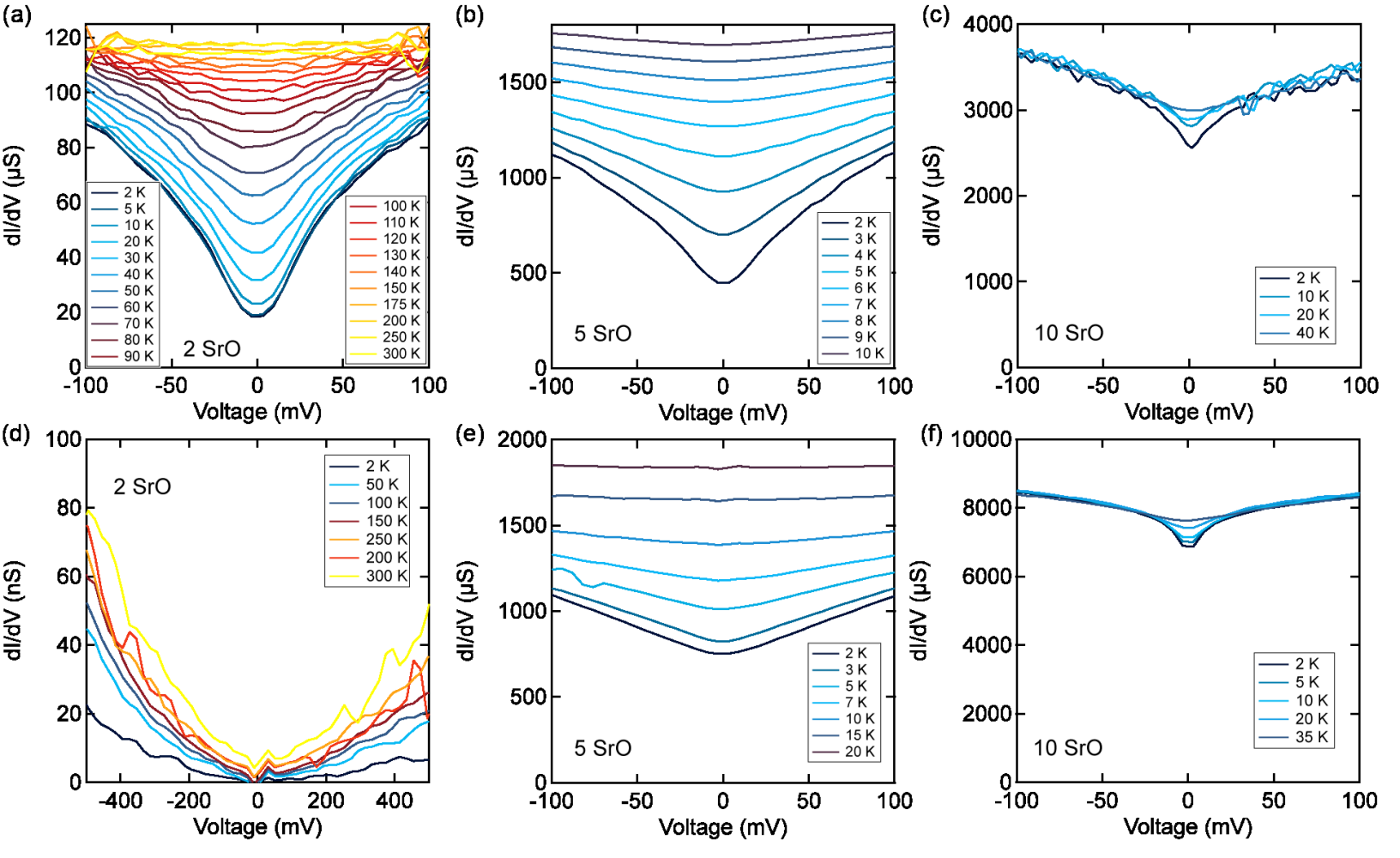
(a)
dI/dV (μS)
Voltage (mV)
2 SrO
2 K
5 K
10 K
20 K
30 K
40 K
50 K
60 K
70 K
80 K
90 K
100 K
110 K
120 K
130 K
140 K
150 K
175 K
200 K
250 K
300 K
(b)
dI/dV (μS)
Voltage (mV)
5 SrO
2 K
3 K
4 K
5 K
6 K
7 K
8 K
9 K
10 K
(c)
dI/dV (μS)
Voltage (mV)
10 SrO
2 K
10 K
20 K
40 K
(d)
dI/dV (nS)
Voltage (mV)
2 SrO
2 K
50 K
100 K
150 K
250 K
200 K
300 K
(e)
dI/dV (μS)
Voltage (mV)
5 SrO
2 K
3 K
5 K
7 K
10 K
15 K
20 K
(f)
dI/dV (μS)
Voltage (mV)
10 SrO
2 K
5 K
10 K
20 K
35 K

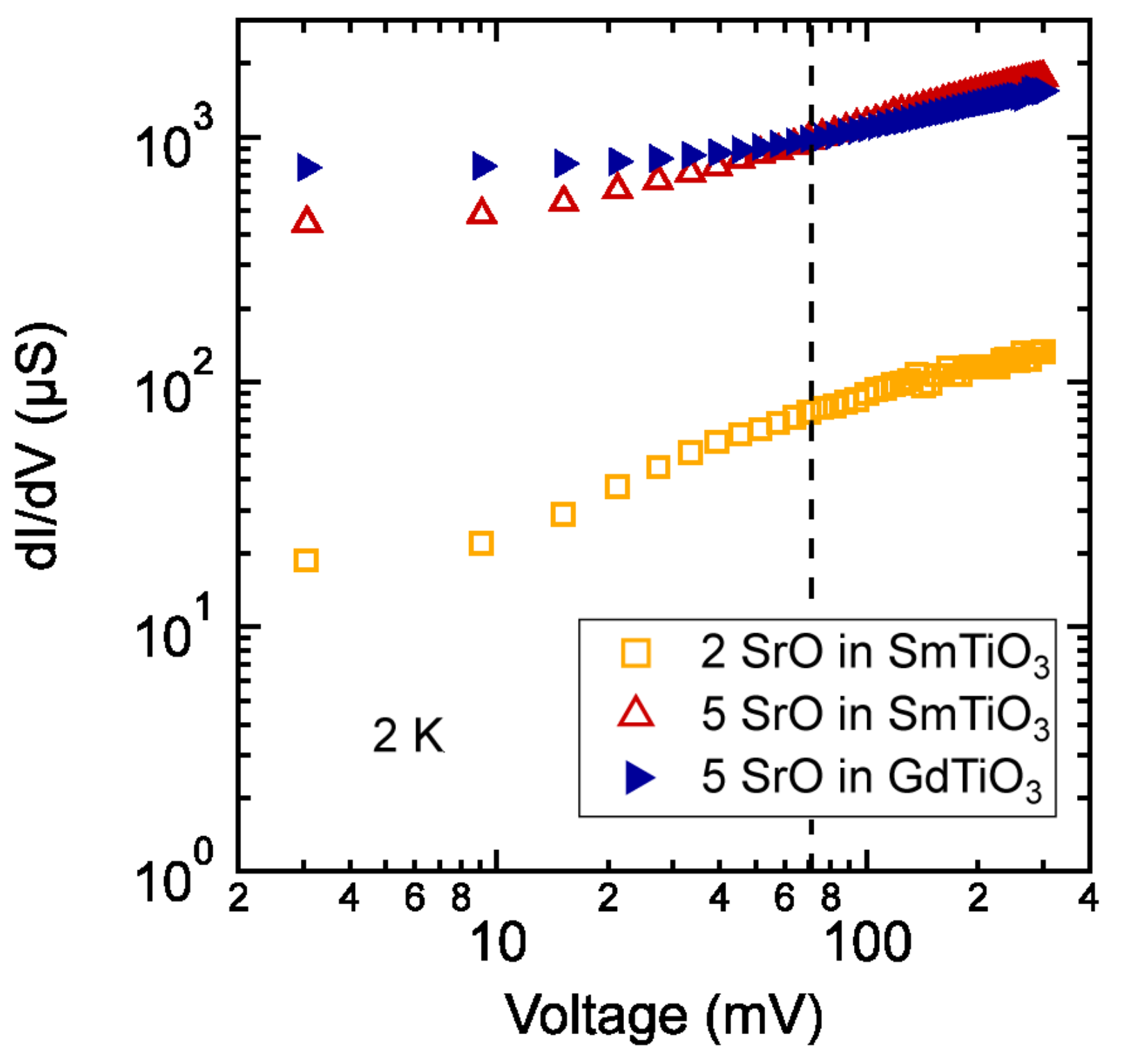
dI/dV (μS)
10^3
10^2
10^1
10^0
2 K
2 SrO in $SmTiO_3$
5 SrO in $SmTiO_3$
5 SrO in $GdTiO_3$
2
4
6
8
10
2
4
6
8
100
2
4
Voltage (mV)

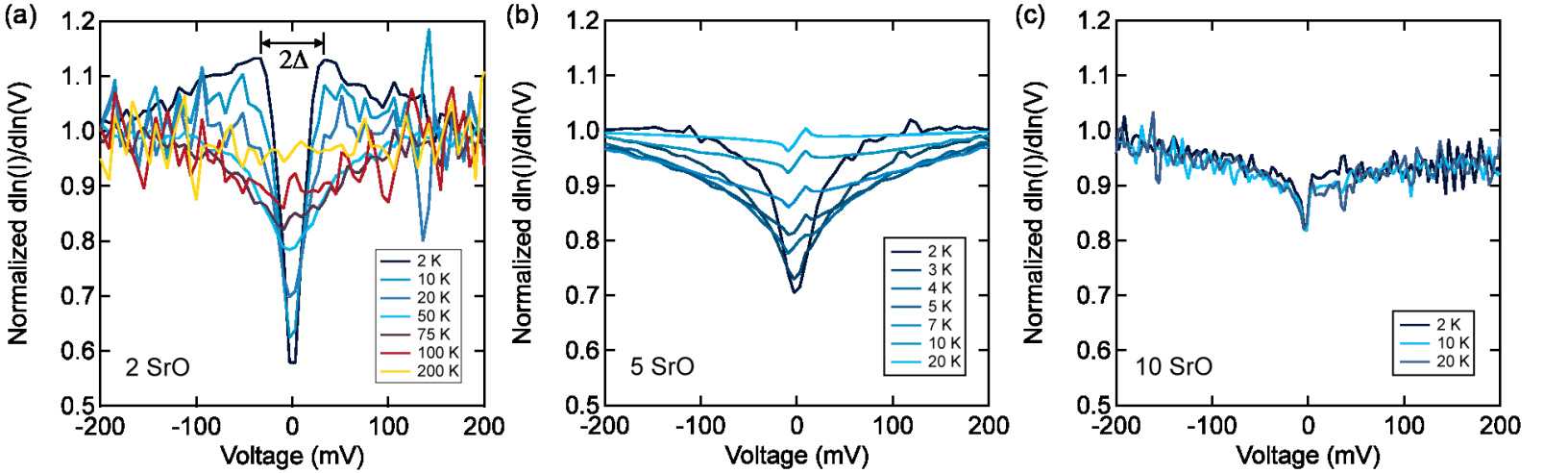
(a)
2Δ
2 SrO
2 K
10 K
20 K
50 K
75 K
100 K
200 K
Normalized dln(I)/dln(V)
Voltage (mV)
(b)
5 SrO
2 K
3 K
4 K
5 K
7 K
10 K
20 K
Normalized dln(I)/dln(V)
Voltage (mV)
(c)
10 SrO
2 K
10 K
20 K
Normalized dln(I)/dln(V)
Voltage (mV)

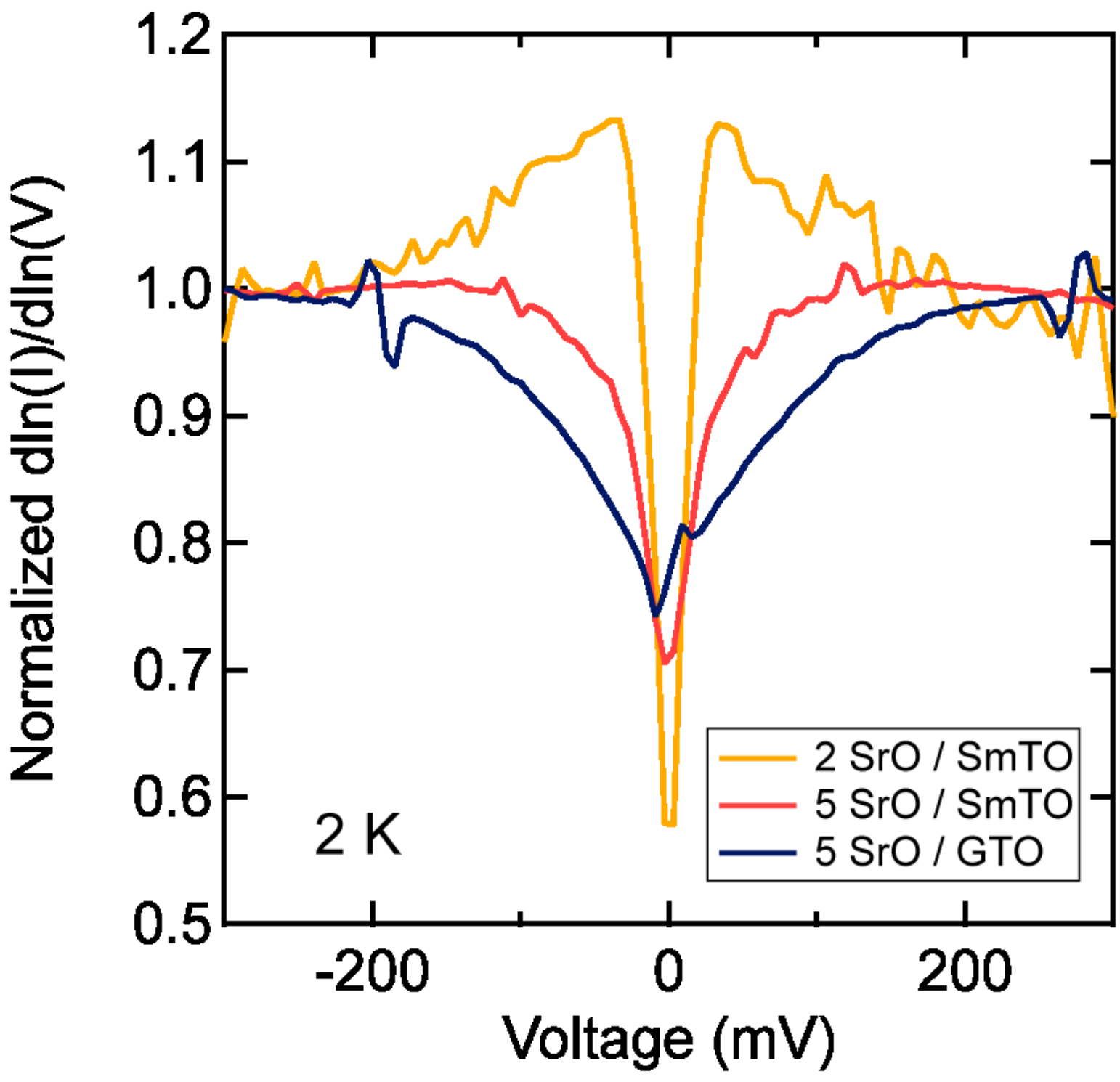
1.2
1.1
1.0
0.9
0.8
0.7
0.6
0.5
Normalized dln(I)/dln(V)
-200
0
200
Voltage (mV)
2 K
2 SrO / SmTO
5 SrO / SmTO
5 SrO / GTO